Optical fiber nanoprobe preparation for near-field optical microscopy by chemical etching under surface tension and capillary action

Samir K. Mondal[1]*, Anupam Mitra[2], Nahar Singh[1], S. N. Sarkar[3], and Pawan Kapur[1]

[1]*Central Scientific Instruments Organisation, Chandigarh, Sec.-30C, India*
(Council of Scientific and Industrial Research, New Delhi, India)
[2]*Birla Institute of Technology and Science, Pilani, Goa Campus, Goa, India*
[3]*Department of Electronic Science, University of Calcutta, 92-A.P.C Road, Kolkata-700 009*
**samirmondal01@gmail.com*

Abstract: We propose a technique of chemical etching for fabrication of near perfect optical fiber nanoprobe (NNP). It uses photosensitive single mode optical fiber to etch in hydro fluoric (HF) acid solution. The difference in etching rate for cladding and photosensitive core in HF acid solution creates capillary ring along core-cladding boundary under a given condition. The capillary ring is filled with acid solution due to surface tension and capillary action. Finally it creates near perfect symmetric tip at the apex of the fiber as the height of the acid level in capillary ring decreases while width of the ring increases with continuous etching. Typical tip features are short taper length (~4 μm), large cone angle (~38°), and small probe tip dimension (<100 nm). A finite difference time domain (FDTD) analysis is also presented to compare near field optics of the NNP with conventional nanoprobe (CNP). The probe may be ideal for near field optical imaging and sensor applications.

OCIS Codes: (230.2285) Fiber devices and optical amplifiers; (180.4243) Near-field microscopy.

References and links

1. M. Ohtsu, "Progress of high-resolution photon scanning tunneling microscopy due to a nanometric fiber probe," J. Lightwave Technol. **13**(7), 1200–1221 (1995).
2. S. Jiang, H. Ohsawa, K. Yamada, T. Pangaribuan, M. Ohtsu, K. Imai, and A. Ikai,"Nanometric scale biosample observation using a photon scanning tunneling microscope," Jpn. J. Appl. Phys. **31**(Part 1, No. 7), 2282–2287 (1992).
3. Y. Saito, and P. Verma, "Imaging and spectroscopy through plasmonic nanoprobe," Eur. Phys. J. Appl. Phys. **46**(2), 20101 (2009).
4. T. Vo-Dinh, P. Kasili, and M. Wabuuyele, "Nanoprobes and nanobiosensors for monitoring imaging individual living cells," Nanomedicine: NBM **2**, 22–30 (2006).
5. M. Chaigneau, G. Ollivier, T. Minea, and G. Louarn, "Nanoprobes for near-field optical microscopy manufactured by substitute-sheath etching and hollow cathode sputtering," Rev. Sci. Instrum. **77**(10), 103702 (2006).
6. Turner D.R., United States Patent, 4,469,554, AT&T Bell Laboratories, Murray Hill, NJ, USA, 1983.
7. S. Mononobe, and M. Ohtsu, "Fabrication of a pencil-shaped fiber probe for near-field optics by selective chemical etching," J. Lightwave Technol. **14**(10), 2231–2235 (1996).
8. R. Stöckle, C. Fokas, V. Deckert, R. Zenobi, B. Sick, B. Hecht, and U. P. Wild,"High-quality near-field optical probes by tube etching," Appl. Phys. Lett. **75**(2), 160–162 (1999).
9. K. W. C. Lai, C. C. H. Kwong, and W. J. Li, "KL Probes for Robotic-Based Cellular Nano Surgery", in *Proceedings of IEEE Conference on* Nanotechnology (Institute of Electrical and Electronics Engineers, 2003), pp. 152–155.
10. S. T. Huntington, B. C. Gibson, J. Canning, K. Digweed-Lyytikäinen, J. D. Love, and V. Steblina, "A fractal-based fibre for ultra-high throughput optical probes," Opt. Express **15**(5), 2468–2475 (2007), http://www.opticsinfobase.org/oe/abstract.cfm?URI=oe-15-5-2468.

#115108 - $15.00 USD Received 31 Jul 2009; revised 26 Aug 2009; accepted 15 Sep 2009; published 13 Oct 2009

11. T. J. Antosiewicz, and T. Szoplik, "Corrugated metal-coated tapered tip for scanning near-field optical microscope," Opt. Express **15**(17), 10920–10928 (2007), http://www.opticsinfobase.org/oe/abstract.cfm?URI=oe-15-17-10920.
12. V. F. Dryakhlushin, V. P. Veiko, and N. B. Voznesenskii, "Scanning near-field optical microscopy and near-field optical probes: properties, fabrication, and control of parameters," Quantum Electron. **37**(2), 193–203 (2007).
13. C. W. Extrand, and S. I. Moon, "Critical meniscus height of liquids at the circular edge of cylindrical rods and disks," Langmuir **25**(2), 992–996 (2009).
14. K. S. Birdi, D. T. Vu, A. Winter, and, A. Norregard, "Capillary rise of liquids in rectangular tubings," Colloid Polym. Sci. **266**, 470–474 (1988).
15. Allen Taflove and Susan C. Hagness, *Computational Electrodynamics: The Finite-Difference Time-Domain Method* (Artech: Norwood, MA, 2000).
16. S. S. Wang, J. Fu, M. Qiu, K. J. Huang, Z. Ma, and L. M. Tong, "Modeling endface output patterns of optical micro/nanofibers," Opt. Express **16**(12), 8887–8895 (2008), http://www.opticsinfobase.org/oe/abstract.cfm?URI=oe-16-12-8887.
17. A. Farjadpour, D. Roundy, A. Rodriguez, M. Ibanescu, P. Bermel, J. D. Joannopoulos, S. G. Johnson, and G. W. Burr, "Improving accuracy by subpixel smoothing in the finite-difference time domain," Opt. Lett. **31**(20), 2972–2974 (2006).

1. Introduction

Study of near field optics shows potential benefits by removing classical diffraction limit of optics. Developing special probing arrangement is a major issue to study near field optics. Nanometric probing in scanning near field optical microscopy (SNOM) [1–5] enables acquisition of optical images with a resolution beyond the Rayleigh diffraction limit by scanning a light source of subwavelength diameter across the sample surface. Nanoprobe has also been using in many studies like biological sample analysis, single molecule imaging, surface plasmonics, and surface enhanced Raman scattering detection. In SNOM employing a probe tip, the apex size of the tip is important that decides the quality of the image. Usually, the probe is a metal coated tapered optical fiber with a tiny tip aperture whose diameter could be between 50 and 200 nm. It is quite difficult to manufacture nanoprobe in a controlled mechanism. The cost-effective and wide application of the scanning near-field optical microscopy can be assured by producing probes with a sufficient accuracy and a good reproducibility. Various techniques on nanoprobe fabrication are reported in published works [6–11]. There are two methods commonly used for the preparation of tapered optical fibers with a sharp tip and reasonable cone angle: (i) heating and pulling [12] method, and (ii) chemical etching in aqueous solution of HF acid. Chemical etching technique is widely used as it achieves fiber tips with much shorter cone and much larger angle, allowing higher transmission. Turner patented [6] a method on fabrication of optical fiber nanoprobe which leads nanoprobe fabrication by chemical etching. The method is based on glass fiber etching guided with surface tension meniscus rise of HF acid solution along the fiber. The mechanism is based on the fact that the meniscus height is a function of the remaining fiber diameter. Although it is convenient and cost-effective, one of the shortcomings of this method lies in its sensitivity related to the ambient conditions. Hence, it often leads to imperfections, like axis asymmetry in the probe cone, rough probe surface etc. Such features strongly affect the near-field optical signal. Keeping acrylate jacket of the optical fiber during the etching, known as tube etching [8], into the HF solution improve quality of the probe but difficulty arises to remove the jacket after the tip formation, breakage is significant and probe's length is big.

In this paper we propose a new etching method for fine fiber nanoprobe fabrication. The method is also based on simple chemical etching in HF solution but probe shape is determined by surface tension meniscus rise, and self-etched capillary ring and capillary rise of the acid solution at the fiber core-cladding boundary. It needs special type of optical fiber having faster etching rate for fiber core compared to its cladding. The method is first time reported to the best of our knowledge. The remaining part of the paper is organized as follows.

Section 2 describes etching process and probe fabrication in diagrams with a theoretical explanation. Section 3 presents fabricated nanoprobes and FDTD analysis for near field optics of the nanoprobes. Finally, a conclusion is drawn in section 4.

#115108 - $15.00 USD Received 31 Jul 2009; revised 26 Aug 2009; accepted 15 Sep 2009; published 13 Oct 2009

2. Etching process in steps

The technique presented here is an evolution of chemical etching technique for fiber nanoprobe fabrication. Figure 1 illustrates etching and fabrication procedure in steps. Etching is performed inside a plastic beaker containing glycerin at the bottom. A certain amount of diluted, 48%, HF acid solution is poured into the beaker. The aqueous solution of the acid being lighter floats on glycerin. A small amount of toluene is added into the beaker. Toluene floats on and covers free surface of the acid solution preventing evaporation of the toxic acid. A special type of GeO_2 doped photosensitive single-mode optical fiber of diameter 125 µm with mode field diameter ~7 µm is stripped and dipped inside the acid solution from a stable holder. Due to surface tension force between the acid solution and glass optical fiber a thin film of HF acid rises along the edge of the stripped cylindrical fiber, Fig. 1, Step (I).

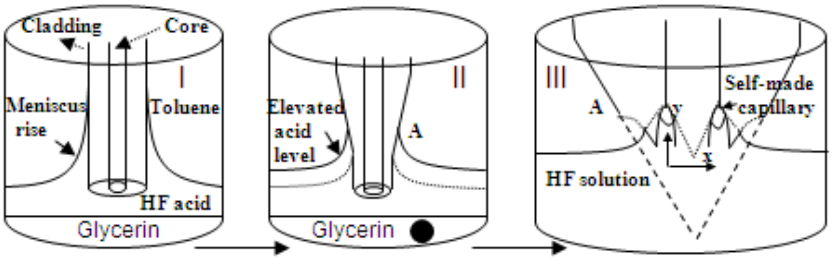

Fig. 1. Schematic illustration of the etching process to fabricate the probe: Step (I) stripped fiber is dipped in acid solution and shows meniscus rise, Step (II) after an interval of ~30 minutes HF acid level is elevated by ~10 µm to 20 µm by dropping steel ball shown in the figure, Step (III) Enlarged picture showing schematic of self-made capillary ring at core-cladding boundary due to different etching rate for core and cladding. Capillary ring controls final probe dimension shown by square dotted line.

It is well known phenomenon that liquid will rise up along the edge of the stripped fiber due to surface tension combined with adhesion to the wall of the fiber. The general balance of capillary and hydrostatic forces and relation between meniscus rise h and radius r of the fiber can be described as [13]

$$h_{Meniscus} = \left[2(\frac{\gamma}{\rho g})(1-\cos\theta_a) \right]^{1/2} \left[1+(\frac{\gamma}{\rho g})^{1/2} \frac{1}{r} \right]^{-1/2} \quad (1)$$

where γ, ρ, *and* θ_a are surface tension, density, and contact angle of the liquid respectively, g is the acceleration due to gravity, and r is the radius of the optical fiber. Although there is no data available on surface tension and contact angle of such solution with silica, it is observed that meniscus rises within 300 µm to 400 µm along the silica fiber of diameter 125 µm depending on the degree of dilution of HF acid. According to the Turner method meniscus etches the fiber producing 300 µm to 400 µm long probe with small cone angle determined by meniscus rise and original fiber diameter. The relation between radius *r* and $h_{Meniscus}$ given in Eq. (1) also determines surface curvature of the respective nanoprobes.

We define CNP for the probe, Fig. 2 (c), made by single step meniscus controlled etching, Step (I), which is also common in this new technique. After a certain period of etching, an intermediate step is introduced where acid level around the fiber is elevated by a small height. The Step (II) in Fig. 1 shows the elevation of the acid level which should be far below the initial meniscus rise in Step (I). As etching approaches towards the core of the fiber, ~30 minutes of etching of the fiber at the etching rate of 3.2 µm/ minute, acid level is elevated by several microns, 10µm – 20 µm, by dropping a solid metallic sphere (steel ball) of appropriate

#115108 - $15.00 USD Received 31 Jul 2009; revised 26 Aug 2009; accepted 15 Sep 2009; published 13 Oct 2009

volume into the beaker. The schematic in Step (II) in Fig. 1 shows elevation of the acid level after dropping steel ball into it. The ball is washed in glycerin to avoid acid contamination. Etching at elevated region should maintain conical shape of the fiber whereas below the elevation regime it etches fiber sidewise preserving its cylindrical shape.

Finally Step (III) in Fig. 1 describes the mechanism of NNP fabrication. As etching solution reaches to the core-cladding boundary it etches fiber core sidewise (x-direction) as well as vertically (y-direction) along core-cladding boundary and form a capillary ring. The elevated acid level favors upward etching and pushes it further above the new acid level due to surface tension pulling along self-made core-cladding capillary ring. Step (III) in Fig. 1 schematically shows formation of self-made circular capillary ring around fiber core-cladding boundary and surface tension capillary rise along the ring. Elevated acid level and difference in the etching rate of fiber cladding and core creates capillary ring at the core-cladding boundary. The final tip shape depends on capillary ring and capillary rise due to surface tension. The capillary rise of HF acid solution in the capillary ring due to surface tension can be expressed as [14]

$$h_{capillary} = \frac{2\gamma}{\rho g r} \cos\theta_a \qquad (2)$$

After attaining a certain height the capillary rise should start falling while ring width increases due to continuous etching resulting a nanoprobe at the apex of the fiber and a circular rim at the base of the probe towards the cladding. The square dotted drawing around the core of the fiber in Step (III) estimates the shape of the final nanoprobe. The relation between $h_{capillary}$ and radius r of the ring given in Eq. (2) should determine surface curvature of NNP.

3. (a) Fabricated probes

Figure 2 (a) and (b) are the SEM pictures of the NNP fabricated by chemical etching technique described above. The probe is coated with few nanometer Aluminum coating for SEM imaging. Uniform coating of Aluminum, as seen in SEM image, suggests that the residual capillary should not pose any difficulty in coating the nanoprobe. The fabricated NNP in Fig. 2 (a) is similar to the predicted tip shown by square dotted line in Step (III) in Fig. 1.

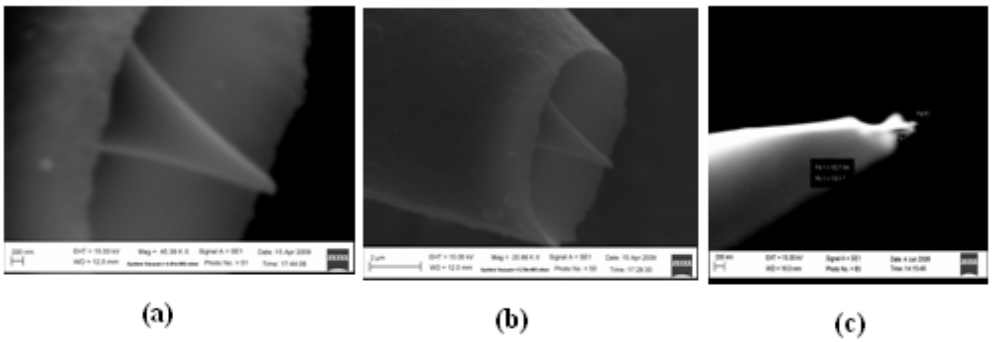

Fig. 2. (a) and (b) are SEM images of NNP with different resolutions, (c) is SEM image of CNP made by single step meniscus rise based chemical etching under similar conditions. The rim at the base of the nanoprobe likely to be part of the capillary ring left after completion of etching. The scale bars are (a) 200 nm, (b) 2µm, and (c) 200 nm.

In absence of elevated acid level, the probe shape should follow pencil like tip shape outlined by dashed line in, Step (III), Fig. 1. It is observed that the near perfect probe has height ~4 µm, base ~3 µm. Introduction of the intermediate Step (II) in Fig. 1 and using photosensitive fiber determine probe's shape. The probe appears perfectly symmetric with large cone angle of 38°. The total taper length is also reduced to ~4 µm form ~350 µm, length

#115108 - $15.00 USD Received 31 Jul 2009; revised 26 Aug 2009; accepted 15 Sep 2009; published 13 Oct 2009

of CNP. Bigger cone angle and short probe length should increase light collection efficiency significantly. Also HF acid being highly corrosive, longer etching period increases chance of deformation in the nanoprobe. We observe one such off-axis deformation in the CNP, Fig. 2(c), made under similar ambient conditions. Although the total etching period is same for both the cases, the effective etching period for NNP is much less and minimizes probe deformation. We also observe a difference in the surface curvature of NNP and CNP. The surface curvature on the NNP is determined by the rectangular hyperbolic relation, hr = constant, between height (h) and radius (r) of the capillary rise given in Eq. (2). Figure 2 (a) shows that the probe surface gets an inwards curvature although radius of curvature is very large. The NNP curvature appears visibly different from the surface curvature of CNP which is determined by Eq. (1). The rim like capillary boundary at the base of the nanoprobe is part of the capillary ring left after the completion of etching. It has shorter height than nanoprobe as surface tension rise toward cladding side of the capillary ring will be dominating due to bigger outer radius which results in longer meniscus rise (Eq. (1)). The rim at the base, smaller dimensions and surface curvature of the NNP are the evidences for capillary rise factor in making the nanoprobe.

b. FDTD analysis

The FDTD simulation demonstrates near field optics characteristics of uncoated NNP and CNP at the end of single-mode optical fibers. Figure 3 presents FDTD simulation results for field propagation and light throughput capacity of the probes. The simulation is performed using the FDTD method [15] and Meep with subpixel smoothing for increased accuracy [16,17]. The base diameter and length of NNP and CNP are taken as 3µm and 4 µm, and 125 µm and 300 µm respectively [5]. The dimensions for NNP are taken from its SEM image. For FDTD simulation of NNP, a uniform grid of 1280 × 1280 × 1280 is taken along the *x*, *y* and *z* directions for a volume of size 16µm × 16µm × 16µm and for CNP, a uniform grid of 8800 × 8800 × 32000 is taken along *x*, *y* and z for a volume of size 110 µm × 110 µm × 400 µm.

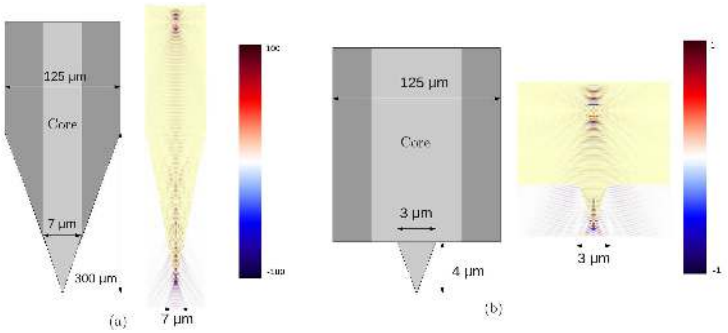

Fig. 3. plots FDTD simulation results for optical field propagation and distribution in fiber with nanoprobes illuminated by similar source but different amplitudes. The adjacent color bars are to estimate magnitude of the field in the probes. The schematic of single-mode fibers (core 7 µm, diameter 125µm) with probe present respective design.

We have taken smaller dimension for NNP to make tip visible in Fig. 3(b). A large dipole source [15] of unit amplitude emitting monochromatic waves at wavelength, λ = 1550 nm is placed inside the fiber with NNP. For the CNP we consider same source but 100 times stronger in amplitude for the FDTD simulation. Figure 3(a) and (b) show field propagation and pattern in CNP and NNP respectively. The color bar and field pattern in the nanoprobes estimate light guidance capacity of the probes.

The simulation does not include the curvature that appears at the boundary of the nanoprobe base as it may not be possible to extract exact information of the curvature. However, it should not change the light collection efficiency as the position of the curvature is far from the nanoprobe base. To study near field characteristics of NNP we compare the

#115108 - $15.00 USD Received 31 Jul 2009; revised 26 Aug 2009; accepted 15 Sep 2009; published 13 Oct 2009

normalized near field distribution of the probes near the tips. The blue and red curves in Fig. 4 present beam width of CNP and NNP respectively measured at 100 nm away from the tip. The normalized power plot reveals that the full-width-half-maxima (FWHM) of NNP, ~200 nm, is ~1/3 of the FWHM for CNP. It is also found that the NNP makes 34 times throughput compared to CNP.

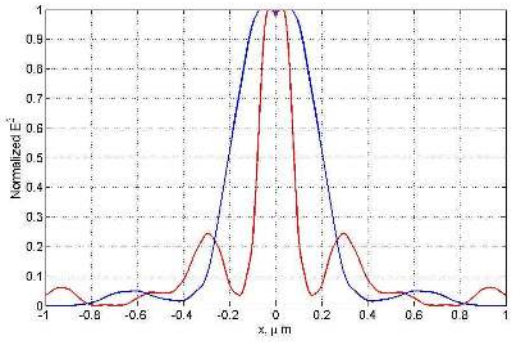

Fig. 4. Normalized near field distribution for NNP (–––) and CNP (–––) at 100 nm from probes tip.

The smaller value of FWHM and enhanced throughput reduces noise level in collected optical signals. Confined and higher throughput should also make NNP potential for sensor probe for Surface Enhanced Raman Scattering (SERS) detection. It is to be mentioned that the near field characteristic of the nanoprobe should be different with nano order metal film coating. However, the FDTD results of the uncoated nanoprobes should be helpful for evaluating the optics of the probe.

4. Conclusions

We propose a new approach of chemical etching for fabricating near perfect optical fiber nanoprobe using GeO_2 doped photosensitive single mode optical fiber. The method is based on chemical etching guided under surface tension capillary rise and surface tension meniscus rise. The fabricated probe has shorter dimensions, base ~3μm and height 4 μm, ideal for near field imaging applications. The probe appears perfectly symmetric about the fiber axis and has bigger cone angle of 38° which enhances light throughput and light collection efficiency. FDTD analysis shows 34 times enhancement in optical throughput compared to CNP. Smaller value of FWHM, ~200 nm, should reduce noise level in collected optical signal. The NNP may be ideal low cost probe for SNOM, SERS detection, and other sensor and imaging applications. The method also needs optimization to control the shape of the tip further.

Acknowledgement

The authors would like to thank the Director, IMTECH, Chandigarh, India for providing the facilities and Mr. Anil Theophilus for technical assistance in SEM experiment. Authors are also thankful to Umesh Tiwari and other staffs of photonics division, CSIO for their co-operation during the work. The authors also thank Dr. H. S. Maiti, Chairman, CSIR Task Force on Photonics for Laser, Communication and Sensor Technology, for the motivation and support to carry out this work under the CSIR Network Project.

#115108 - $15.00 USD Received 31 Jul 2009; revised 26 Aug 2009; accepted 15 Sep 2009; published 13 Oct 2009